AIMS Mathematics, 10(3): 5456–5479.
DOI: 10.3934/math.2025252
Received: 12 December 2024
Revised: 15 February 2025
Accepted: 21 February 2025
Published: 11 March 2025

https://www.aimspress.com/journal/Math

Research article

On the new sine-Gordon solitons of the generalized Korteweg-de Vries and modified Korteweg-de Vries models via beta operator

Yaya Wang[1], **Md Nurul Raihen**[2,4,*], **Esin Ilhan**[3] **and Haci Mehmet Baskonus**[4]

[1] Department of Information Engineering, Binzhou Polytechnic, Binzhou, 256600, China
[2] Department of Mathematics and Statistics, University of Toledo, OH, 43606, USA
[3] Faculty of Engineering and Architecture, Kirsehir Ahi Evran University, Kirsehir, Turkey
[4] Department of Mathematics and Science Education, Harran University, Sanliurfa, Turkey

* **Correspondence:** Email: nurul.raihen@gmail.com; Tel: +1-313-378-7353.

Abstract: In this paper, we applied the sine-Gordon expansion method (SGEM) and the rational sine-Gordon expansion method (RSGEM) for obtaining some new analytical solutions of the (2+1)-dimensional generalized Korteweg-de Vries (gKdV) and modified Korteweg-de Vries (mKdV) equations with a beta operator. The sine-Gordon expansion method (SGEM) has recently been extended to a rational form, referred to as the rational sine-Gordon expansion method (RSGEM). By applying a specific transformation, the equations are reduced to a nonlinear ordinary differential equation (NODE), allowing for the derivation of analytical solutions in various forms, including complex, hyperbolic, rational, and exponential. All these solutions are expressed through periodic functions using SGEM and RSGEM. The physical significance of the parametric dependencies of these solutions is also examined. Additionally, several simulations, including three-diemensional (3D) visualizations and revolutionary wave behaviors, are presented, based on different parameter selections. Revolutionary surfaces, defined by height and radius as independent variables, are extracted to further illustrate the wave dynamics.

Keywords: gKdV equation; mKdV equation; beta operator; analytical method; analytic solutions
Mathematics Subject Classification: 35A24, 35Q53

1. Introduction

Nonlinear partial differential equations (NLPDEs) have been used for people to understand the complex real-world phenomena, as they account for nonlinearity, time, and interactions among multiple independent variables [1]. These equations have often incorporated some parameters, whose values are determined by the specific conditions, making them highly versatile in capturing the

behavior of certain systems [1]. Therefore, as scientific researches and mathematical modeling continue to advance, an increasing number of NLPDEs with both constant and variable coefficients are being introduced, allowing for more accurate and detailed descriptions of intricate physical processes [2]. Over the last several decades, there has been a significant rise in the modeling of various aspects of nonlinear equations [3–5]. Among these, the KdV equation is one of the most renowned, which was first derived in 1895 by Dutch mathematicians Diederik Korteweg and Gustav de Vries [6]. They introduced this equation to model the propagation of long, shallow-water waves with small amplitudes. The equation was originally developed to explain the appearance and persistence of solitary waves, or solitons, which were observed in shallow canals. Especially, in recent years, numerous problems have been represented using mathematical models [7–9]. Various operators and mathematical frameworks have been employed to analyze and explore such problems. Within this context, Bendahmane and his team introduced a new coupled electro-thermo radiofrequency model for cardiac tissue [10]. More recently, mathematical models have been utilized to develop artificial intelligence algorithms for optimizing computer programming [11]. Using artificial neural networks, experts have studied various real-world problems, including the effects of hard water consumption on kidney function and diseases [12], analyzing Hashimoto's thyroiditis [13], predicting the operation of open-sun drying [14], and modeling the nonlinear dynamics of emigration and migration [15]. A new nonlinear fractal fractional mathematical model has been introduced to analyze the spread of malicious codes in wireless sensor networks. This model addresses computer virus-related issues by leveraging the benefits of both fractal and fractional operators [16]. Basit et al. explored a new thermal analysis for heat and mass transfer in bioconvective Carreau nanofluid flowing over an inclined stretchable cylinder [17]. Pandey developed a comprehensive analysis for the efficient and robust control of irrigation canals. That study presents a hydraulic model for irrigation canals, integrating water levels and gate dynamics to improve discharge predictions [18]. Begley conducted studies to explore the deeper properties of endocrine diseases using mathematical modeling and computational methods [19]. Yang et al. investigated the behavior of computer viruses in signal bases, reporting on the application of the Routh-Hurwitz criteria and the Hopf bifurcation theorem in their model [20]. Seddik et al. introduced a new generative mathematical model utilizing binary pixel images to investigate the encryption process in image generation [21]. More recently, a physiological mathematical model was developed to study the human thyroid [22]. Among the most significant epidemiological models is cancer, and a new mathematical model addressing cancer invasion has been explored [23]. In recent decades, these models have been extensively investigated to extract traveling wave solutions. Within this context, analytical solutions were used to study the evolution of non-isothermal pore-pressure in hydrating mine fill [24]. In epidemiological models, 3D temperature fields for skin tissue were analyzed through the application of analytical solutions [25]. Sweilam investigated a novel crossover dynamics model for monkeypox disease using fractional differential equations and the Caputo derivative [26]. Shirole et al. presented a method for predicting the left ventricle ejection fraction from heart rate variability (HRV) in patients with diabetes and cardiac disease [27].

Through these models and studies, mathematical models have been extensively utilized to explore the underlying properties of real-world problems [28–31]. Therefore, examining analytic solutions of these models plays a crucial role in analyzing physical problems, as it helps evaluate the accuracy of approximations, numerical methods, and computational programs. Consequently, developing efficient and effective methods for obtaining analytic solutions is crucial to enhancing the utility of such

computations. These computational techniques have become essential across a range of scientific disciplines, including financial mathematics, aerospace, quantum physics, and environmental studies. As a result, the advancement of new computational techniques for solving NLPDEs models and their applications is essential for scientific and technological progress.

In this regards, we will study the gKdV and mKdV equations using the beta derivative operator as follows [32]:

$$D_t^{\beta} u(x, y, t) = auu_x - auu_y + bu_{xxx} - bu_{yyy} - cu_{xxy} + cu_{xyy}, \tag{1.1}$$

$$D_t^{\beta} u(x, y, t) = au^2u_x - au^2u_y + bu_{xxx} - bu_{yyy} - cu_{xxy} + cu_{xyy}, \tag{1.2}$$

where a, b, and c are real constants; $0 < \beta \leq 1$; and $u(x, y, t)$ is the dependent variable that represents the wave profile. Equations (1.1) and (1.2) were studied by Wang and Kara [33], who applied Lie group theory to analyze them, deriving several invariant solutions. Subsequently, Wazwaz [34] demonstrated the integrability of these equations using the Painlevé test and obtained soliton solutions. Kumar and Malik [35] employed the Kudryashov technique to generate bright and singular soliton solutions for the same equations. Yuan [36] investigated the combined KdV-mKdV equation using a bilinear approach and developed rational solutions incorporating free multi-parameters. Ali [37] conducted an analysis of these equations to generate solitary wave solutions. Ahmad [38] developed an explicit difference method to derive waveform soliton solutions for the KdV and mKdV equations. Additionally, Elmandouha and Ibrahim [39] used the dynamic system approach to explore bifurcations and derive analytic traveling wave solutions for the KdV equation (1.1).

The KdV equation has been widely utilized to model various phenomena in physics and engineering. It is particularly useful in the study of magnetoacoustic wave propagation, small-amplitude shallow-water waves, fluid and plasma turbulence, and shock wave dynamics. Additionally, the KdV equation is used to solve complex mathematical problems, such as the determination of gravity waves' speed, and in many physical phenomena including electrohydrodynamic flows, acoustic waves in nonuniform atmospheric conditions, and the transmission of optical solitons in fiber optics, among many others [40, 41]. Due to its robustness in modeling nonlinear wave phenomena, the KdV equation has become an essential tool for researchers working in various scientific fields. Throughout the years, the KdV equation has been a fundamental tool in mathematical analyses and modeling for physics and engineering, showcasing the remarkable ability of mathematics to predict and unravel complex physical behaviors. Its continued relevance underscores the importance of mathematical frameworks in advancing our understanding of intricate real-world phenomena. At the same time, various KdV extensions are being developed [42–44]. The wide range of KdV applications and numerous KdV extensions have become invaluable tools for many professionals [45, 46]. Ongoing researches and developments ensure that those extensions/generalizations will continue to play a vital role in scientific progress [45, 46].

In the following, we propose some analytical solutions of Eqs (1.1) and (1.2) based on the SGEM and RSGEM. The RSGEM method is newly developed and, to the best of our knowledge, it has not yet been applied to the nonlinear (2+1)-dimensional gKdV and mKdV equations in any published work. This paper introduces and demonstrates the use of RSGEM, extending the SGEM by incorporating rational trigonometric functions. While the SGEM employs straightforward expansions using trigonometric and hyperbolic functions to derive solutions, the RSGEM incorporates rational trigonometric and hyperbolic forms, allowing for a richer set of solutions, including mixed modes

and more intricate waveforms. This structural enhancement makes the RSGEM capable of addressing more complex wave dynamics and uncovering solutions with singularities or complex patterns, which are not accessible through the SGEM. Additionally, the RSGEM leads to more intricate algebraic systems that require greater computational effort but provide diverse solution types, such as mixed hyperbolic, trigonometric, and exponential forms. Using these approaches, we successfully construct analytic solutions in various forms, including complex functions, hyperbolic functions, trigonometric functions, and exponential functions.

The structure of this paper is as follows: Section 2 provides preliminary remarks on the beta operator. Section 3 outlines the foundational steps of the SGEM and RSGEM. Section 4 focuses on the applications of these methods to derive new analytical traveling wave solutions for the gKdV and mKdV equations. In Section 5, we discuss the physical comments of the obtained results. Finally, Section 6 concludes the paper by highlighting the key contributions and novelties of this work.

2. Preliminaries

This section presents the fundamental definitions related to the beta derivative operator. Let $f(x)$ be a function of all non-negative values of x with the beta derivative, which is defined as follows [47,48]:

$$D_x^{\beta}(f(x)) = \frac{d^{\beta}f(x)}{dx^{\beta}} = \lim_{\delta\to 0}\frac{f\left(x+\delta(x+\frac{1}{\Gamma(\beta)})^{1-\beta}\right)-f(x)}{\delta}, \quad 0<\beta\leq 1, \tag{2.1}$$

where $\Gamma(\beta)$ is the gamma function, defined as

$$\Gamma(x) = \int_0^{\infty} e^{-t}t^{x-1}\,dx. \tag{2.2}$$

Some useful properties are provided as follows [49,50]:

$$D_x^{\beta}(f(x)) = \left(x+\frac{1}{\Gamma(\beta)}\right)^{1-\beta}\frac{df(x)}{dx}. \tag{2.3}$$

$$D_x^{\beta}(fog(x)) = \left(x+\frac{1}{\Gamma(\beta)}\right)^{1-\beta}g'(x)f'(g(x)). \tag{2.4}$$

3. Methodological framework

In this section, the general properties of the SGEM and RSGEM are discussed. Let us consider the sine-Gordon equation, [51–53], which is given as

$$v_{xx} - v_{tt} = m^2\sin(v), \tag{3.1}$$

where $v = v(x,t)$ and $m \in \mathbb{R}\setminus\{0\}$.

Performing the wave transformation $v = V(\eta)$, $\eta = \mu(x-ct)$ upon Eq (3.1), yields the following nonlinear ordinary differential equation (NODE):

$$V'' = \frac{m^2}{\mu^2(1-c^2)}\sin(V), \tag{3.2}$$

in which $V = V(\eta)$, η is the amplitude, and c is the speed of the traveling wave. Integrating Eq (3.2), we get the following equation:

$$\left[\left(\frac{V}{2}\right)'\right]^2 = \frac{m^2}{\mu^2(1-c^2)}\sin^2\left(\frac{V}{2}\right) + K, \tag{3.3}$$

where K is the constant of integration. Putting $K = 0$, $\omega(\eta) = \frac{V}{2}$, and $a^2 = \frac{m^2}{\mu^2(1-c^2)}$ in Eq (3.3), gives:

$$\omega' = a\sin(\omega). \tag{3.4}$$

Substituting $a = 1$ in Eq (3.4), we get,

$$\omega' = \sin(\omega). \tag{3.5}$$

After simplifying Eq (3.5), we have the following two equations:

$$\sin(\omega) = \sin(w(\xi)) = \left.\frac{2pe^{\xi}}{1+p^2e^{2\xi}}\right|_{p=1} = \operatorname{sech}(\xi), \tag{3.6}$$

$$\cos(\omega) = \cos(w(\xi)) = \left.\frac{p^2e^{2\xi}-1}{p^2e^{2\xi}+1}\right|_{p=1} = \tanh(\xi), \tag{3.7}$$

where p is the constant of integration.

3.1. The sine-Gordon method

Let us consider a general nonlinear partial differential equation as follows:

$$P(u, D_t^{\beta}u, u_{xt}, u^2, \cdots) = 0. \tag{3.8}$$

Using the wave transformation $u = u(x,t) = U(\xi)$, $\xi = x - \frac{\lambda}{\beta}\left(t + \frac{1}{\Gamma(\beta)}\right)^{\beta}$, we obtain a nonlinear ordinary differential equation

$$N(U, U', U'', U^2, \cdots) = 0, \tag{3.9}$$

where $U = U(\xi)$, $U' = \frac{dU}{d\xi}$, $U'' = \frac{d^2U}{d\xi^2}, \cdots$. In this model, we consider the trial solution formula as follows:

$$U(\xi) = \sum_{i=1}^{n}\tanh^{i-1}(\eta)[B_i\operatorname{sech}(\eta) + A_i\tanh(\eta)] + A_0. \tag{3.10}$$

Taking Eqs (3.6) and (3.7) into (3.10), we may rewrite it as follows:

$$U(\omega) = \sum_{i=1}^{n}\cos^{i-1}(\omega)[B_i\sin(\omega) + A_i\cos(\omega)] + A_0. \tag{3.11}$$

We determine the value of n is using the balance principle according to the terms of the NODE (obtained from Eq (3.8)). When we put Eq (3.11) and its necessary derivation in Eq (3.9), we derive a set of algebraic equations by summing the coefficients of $\sin^i(\omega)\cos^j(\omega)$ with the same power and setting each sum to zero. We use symbolic computation to simplify the set of algebraic equations, allowing us to determine the values of the coefficients A_i, B_i, μ, and c. Finally, by substituting the values of A_i, B_i, μ, and c into Eq (3.10), we obtain new traveling wave solutions to Eq (3.8).

3.2. The rational sine-Gordon method

Let us consider a general nonlinear partial differential model given as follows [30]:

$$P(\Xi, D_t^{\beta}\Xi, \Xi_{xt}, \Xi^2, \cdots) = 0. \tag{3.12}$$

Via $\Xi = \Xi(x,t) = U(\xi)$, $\xi = x - \frac{\lambda}{\beta}\left(t + \frac{1}{\Gamma(\beta)}\right)^{\beta}$, we obtain the nonlinear ordinary differential equation

$$N(U, U', U'', U^2, \cdots) = 0, \tag{3.13}$$

where $U = U(\xi)$, $U' = \frac{dU}{d\xi}, U'' = \frac{d^2U}{d\xi^2}, \cdots$. In this model, we assume the trial solution function to be the following

$$U(\xi) = \frac{\sum_{i=1}^{N} \tanh^{i-1}(\xi)[A_i \mathrm{sech}(\xi) + c_i \tanh(\xi)] + A_0}{\sum_{i=1}^{M} \tanh^{i-1}(\xi)[B_i \mathrm{sech}(\xi) + d_i \tanh(\xi)] + B_0}. \tag{3.14}$$

The resulting solution will be obtained by computing the rational coefficients, and the corresponding method is known as the RSGEM. With the help of Eqs (3.6) and (3.7), Eq (3.14) may be rewritten as

$$U(\omega) = \frac{\sum_{i=1}^{N} \cos^{i-1}(\omega)[A_i \sin(\omega) + c_i \cos(\omega)] + A_0}{\sum_{i=1}^{M} \cos^{i-1}(\omega)[B_i \sin(\omega) + d_i \cos(\omega)] + B_0}. \tag{3.15}$$

The balances M and N are obtained. When we substitute Eq (3.14) and its necessary derivation in Eq (3.13), we obtain an algebraic equation. By solving this equation, we find the values of the parameters given by Eq (3.15). If we put these values into Eq (3.14), we find some new analytical solutions of Eq (3.12).

4. Applications

In this part of the paper, we apply the SGEM and RSGEM to obtain new analytical solutions for the (2+1)-dimensional gKdV and mKdV systems, as detailed below.

4.1. SGEM solution of the (2+1)-dimensional generalized KdV equation

In this subsection, multiple analytical solutions to the gKdV equation (1.1) are extracted using SGEM. For simplicity, the following transformation of the dependent variables is considered:

$$u(x, y, t) = U(\xi), \tag{4.1}$$

where

$$\xi = x + ky + \frac{w}{\beta}\left(t + \frac{1}{\Gamma(\beta)}\right)^{\beta}, \quad 0 < \beta \leq 1, \tag{4.2}$$

which results in

$$2(bk^3 - ck^2 + ck - b)U'' + a(k-1)U^2 + 2wU = 0, \tag{4.3}$$

where $U = U(\xi)$, k and w are real nonzero constants. In Eq (4.3), by using the balance principle, we obtain $N = 2$. So, using Eq (3.11), the test function for the solution formula can be expressed as follows:

$$U(\omega) = A_0 + \cos(\omega)A_1 + \cos^2(\omega)A_2 + \sin(\omega)B_1 + \cos(\omega)\sin(\omega)B_2. \tag{4.4}$$

When we substitute Eq (4.4) and its second derivative into Eq (4.3), we derive an algebraic equation involving trigonometric functions. Thus, by equating the coefficients of similar terms, we obtain a system of equations for the parameters. Solving this system allows us to determine the values of parameters such as $A_0, B_1, A_1, B_2, A_2, k$, and w. Substituting these values into Eq (3.10), we obtain the following:

Case 1. The first coefficients are selected as follows:

$$\begin{aligned} A_0 &= \frac{-4ck + 4b(1 + k + k^2)}{a}, A_1 = 0, A_2 = \frac{6ck - 6b(1 + k + k^2)}{a}, B_1 = 0, \\ B_2 &= -\frac{6i(-ck + b(1 + k + k^2))}{a}, w = (-1 + k)(-ck + b(1 + k + k^2)), \end{aligned} \tag{4.5}$$

which yields the following mixed complex singular solution to the system of Eq (1.1):

$$u_1(x, y, t) = \tau \left(-1 - \frac{3i}{-i + \sinh\left[x + ky + \frac{(-1+k)(-ck+b(1+k+K^2))\left(t+\frac{1}{\Gamma(\beta)}\right)^{\beta}}{\beta} \right]} \right), \tag{4.6}$$

where $\tau = \frac{2(-ck+b(1+k+k^2))}{a}$, and $0 < \beta \leq 1$ for the strain condition for the valid solution of the β derivative operator. The wave dynamics of the imaginary part of Eq (4.6) are illustrated through revolutionary graphs in Figure 1 and 3D simulations in Figure 2. These simulations represent a novel contribution to the existing literature.

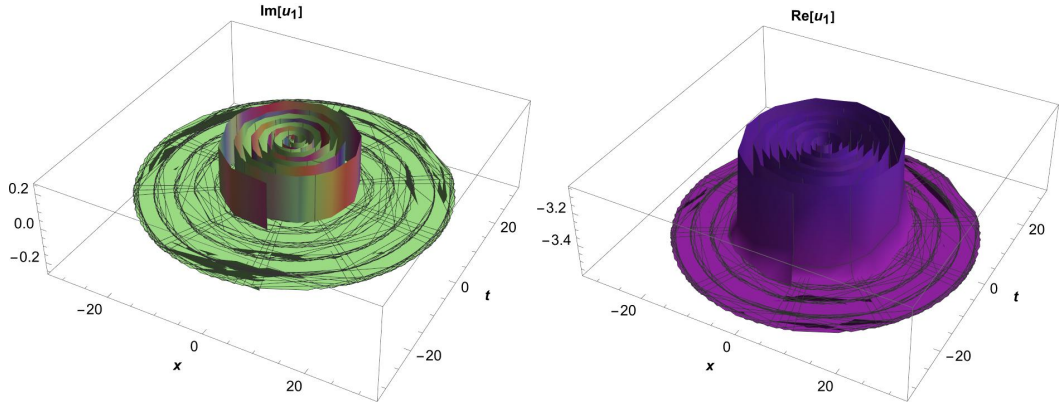

Figure 1. The revolutionary wave behavior of Eq (4.6) for the specified values $k = 0.1, c = 0.2, b = 0.5, a = 0.3, y = 1$, and $\beta = 0.99$.

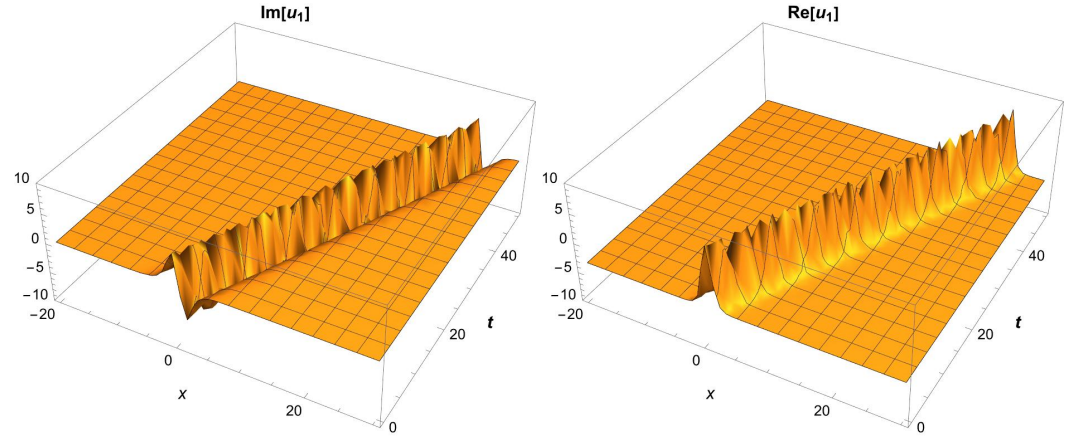

Figure 2. Three-dimensional wave behavior of Eq (4.6) for the specified values $k = 0.1, c = 0.2, b = 0.5, a = 0.3, y = 1$, and $\beta = 0.99$.

Case 2. We select the following coefficients:

$$A_0 = \frac{2iB_2}{3}, A_1 = 0, A_2 = -iB_2, B_1 = 0, b = \frac{6ck + iaB_2}{6(1 + k + k^2)}, w = \frac{1}{6}ia(-1 + k)B_2, \tag{4.7}$$

which gives the following mixed complex rational solution:

$$u_2(x, y, t) = \frac{B_2}{3}\left(-i + \frac{3}{-i + \sinh\left[x + ky + \frac{ia(-1+k)\left(t+\frac{1}{\Gamma(\beta)}\right)^{\beta} B_2}{6\beta}\right]}\right), \tag{4.8}$$

with $0 < \beta \leq 1$ as the strain condition for a valid solution. The wave dynamics of the imaginary part of Eq (4.8) are depicted as revolutionary graphs in Figure 3.

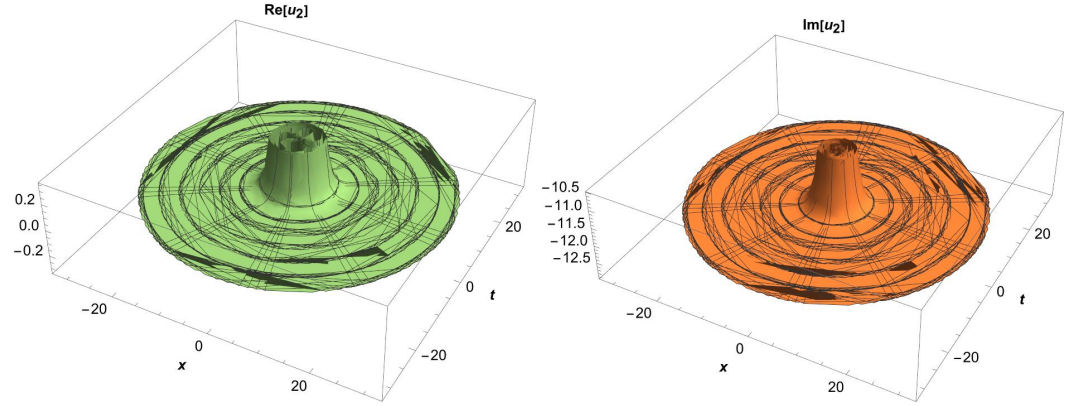

Figure 3. The revolutionary wave behavior of Eq (4.8) for the specified values $a = 0.1, k = 0.2, B_2 = 36, y = 1$, and $\beta = 0.99$.

Case 3. By taking the coefficients

$$A_0 = -\frac{2A_2}{3}, A_1 = 0, B_1 = 0, B_2 = -iA_2, c = \frac{6b(1+k+k^2)+aA_2}{6k}, w = -\frac{1}{6}a(-1+k)A_2, \tag{4.9}$$

we obtain the other complex solution to Eq (1.1) as follows:

$$u_3(x,y,t) = \frac{A_2}{3}\left(1 - \frac{3i}{i + \sinh\left[x + ky - \frac{a(-1+k)\left(t+\frac{1}{\Gamma(\beta)}\right)^{\beta} A_2}{6\beta}\right]}\right), \tag{4.10}$$

where $0 < \beta \leq 1$. Figure 4 presents the two-dimensional (2D) simulations of Eq (4.10).

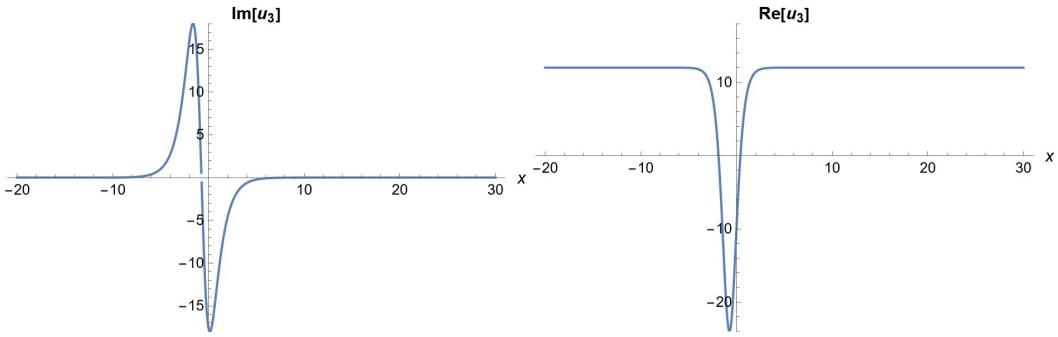

Figure 4. The 2D dynamics of Eq (4.10) for $a = 0.1, k = 0.2, A_2 = 36, y = 1$, and $\beta = 0.99$.

Case 4. When the following coefficients are considered:

$$A_0 = -\frac{2A_2}{3}, A_1 = 0, B_1 = 0, B_2 = -iA_2, a = \frac{6(-1)^{2/3}c}{A_2}, k = (-1)^{2/3}, w = i\sqrt{3}c, \tag{4.11}$$

the other complex solution to Eq (1.1) is obtained as:

$$u_4(x,y,t) = \frac{A_2}{3}\left(1 - \frac{3i}{i + \sinh\left[x + (-1)^{2/3}y + \frac{i\sqrt{3}c\left(t+\frac{1}{\Gamma(\beta)}\right)^{\beta}}{\beta}\right]}\right), \tag{4.12}$$

where $0 < \beta \leq 1$. Figure 5 displays the 2D simulations for Eq (4.12).

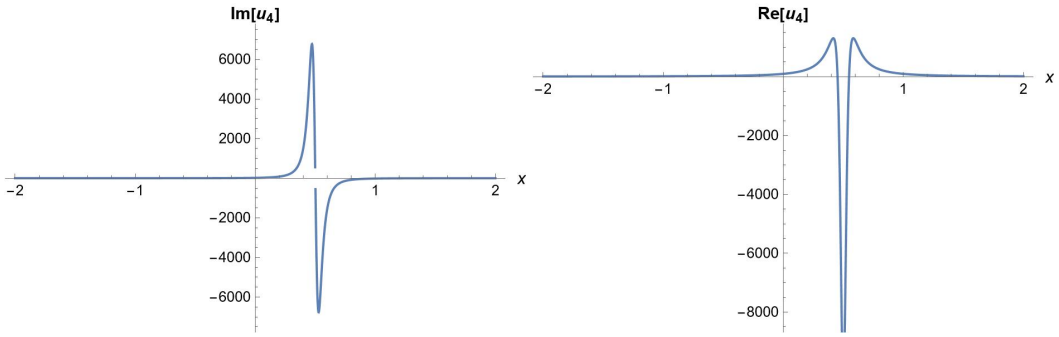

Figure 5. The 2D dynamics of Eq (4.12) for $a = 0.1, A_2 = 12, y = 1, c = 2$, and $\beta = 0.99$.

4.2. SGEM solution of the (2+1)-dimensional mKdV equation

In this subsection, multiple analytical solutions to the mKdV equation (1.2) are obtained using SGEM. To enhance the efficiency of the derivation, we apply the following transformation to the dependent variables:

$$u(x, y, t) = U(\xi), \tag{4.13}$$

where

$$\xi = x + ky + \frac{w}{\beta}\left(t + \frac{1}{\Gamma(\beta)}\right)^{\beta}, \quad 0 < \beta \leq 1, \tag{4.14}$$

yields

$$3(bk^3 - ck^2 + ck - b)U'' + a(k-1)U^3 + 3wU = 0, \tag{4.15}$$

where $U = U(\xi)$, and k and w are real, non-zero constants. Applying the balance principle to Eq (4.15), we determine that $N = 1$. Therefore, using Eq (3.11), the test function for the solution can be written as follows:

$$U(\omega) = A_0 + \sin(\omega)B_1 + \cos(\omega)A_1. \tag{4.16}$$

When Eq (4.16) and its second derivative are substituted into Eq (4.15), an algebraic equation involving trigonometric functions is obtained. Equating the coefficients of corresponding terms yields a system of equations for the parameters. Solving this system provides the values for A_0, B_1, A_1, k, and w. Inserting these values into Eq (3.10) gives the following result.

Case 1. The coefficients are chosen as follows:

$$A_0 = 0, A_1 = \frac{(-1)^{2/3}\sqrt{\frac{3}{2}}\sqrt{c}}{\sqrt{a}}, B_1 = \frac{(-1)^{1/6}\sqrt{3}\sqrt{c}}{\sqrt{2}\sqrt{a}}, k = -(-1)^{1/3}, w = -\frac{1}{2}i\sqrt{3}c, \tag{4.17}$$

which results in the following mixed complex solution for the system of Eq (1.2):

$$u_1(x, y, t) = \frac{(-1)^{1/6}\sqrt{3}\sqrt{c}\left(\operatorname{sech}\left[x - (-1)^{1/3}y - \frac{i\sqrt{3}c}{2\beta}(t + \frac{1}{\Gamma(\beta)})^{\beta}\right] - i\tanh\left[x - (-1)^{1/3}y - \frac{i\sqrt{3}c}{2\beta}(t + \frac{1}{\Gamma(\beta)})^{\beta}\right]\right)}{\sqrt{2}\sqrt{a}}, \tag{4.18}$$

for $0 < \beta \leq 1$, which defines the strain condition for the fractional derivative operator. The wave behavior of the imaginary part of Eq (4.18) is visualized through the revolutionary plots in Figure 6.

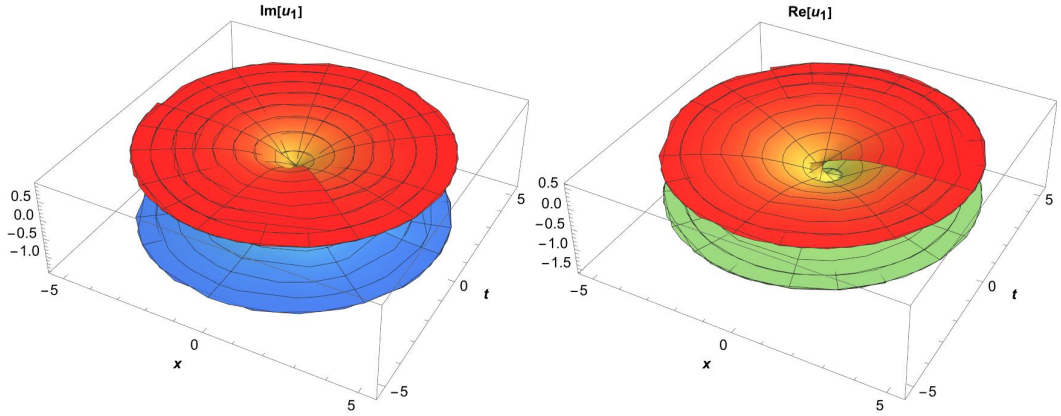

Figure 6. The revolutionary wave behavior of Eq (4.18) for the specified values $c = 0.2, a = 0.3, y = 1$, and $\beta = 0.99$.

Case 2. By choosing the following coefficients

$$A_0 = 0, B_1 = -iA_1, c = b(1 + \frac{1}{k} + k) + \frac{2aA_1^2}{3k}, w = -\frac{1}{3}a(-1 + k)A_1^2, \tag{4.19}$$

we get the mixed complex solution to Eq (1.2) as follows:

$$\begin{aligned} u_2(x, y, t) = A_1\Bigg(- i\,\mathrm{sech}\left[x + ky - \frac{A_1^2}{3\beta}a(-1 + k)\left(t + \frac{1}{\Gamma(\beta)}\right)^{\beta}\right] + \\ \tanh\left[x + ky - \frac{A_1^2}{3\beta}a(-1 + k)\left(t + \frac{1}{\Gamma(\beta)}\right)^{\beta}\right]\Bigg), \end{aligned} \tag{4.20}$$

with $0 < \beta \leq 1$, as the strain condition for a valid solution. The wave dynamics of the imaginary part of Eq (4.20) are illustrated through revolutionary plots and 3D visualizations in Figures 7 and 8, respectively.

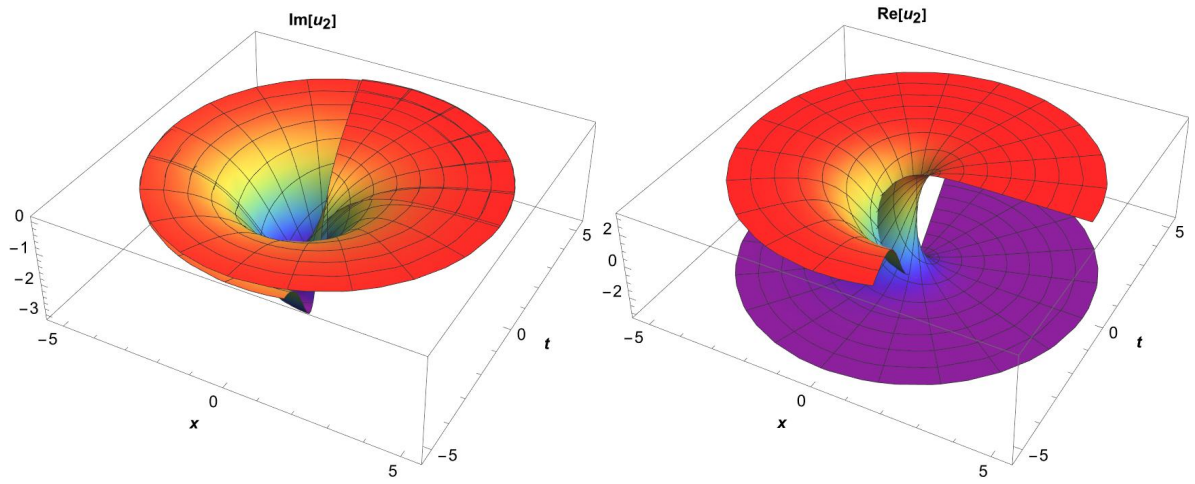

Figure 7. The revolutionary wave behavior of Eq (4.20) for the specified values $k = 2, A_1 = 3, c = 0.2, a = 0.23, y = 1$, and $\beta = 0.99$.

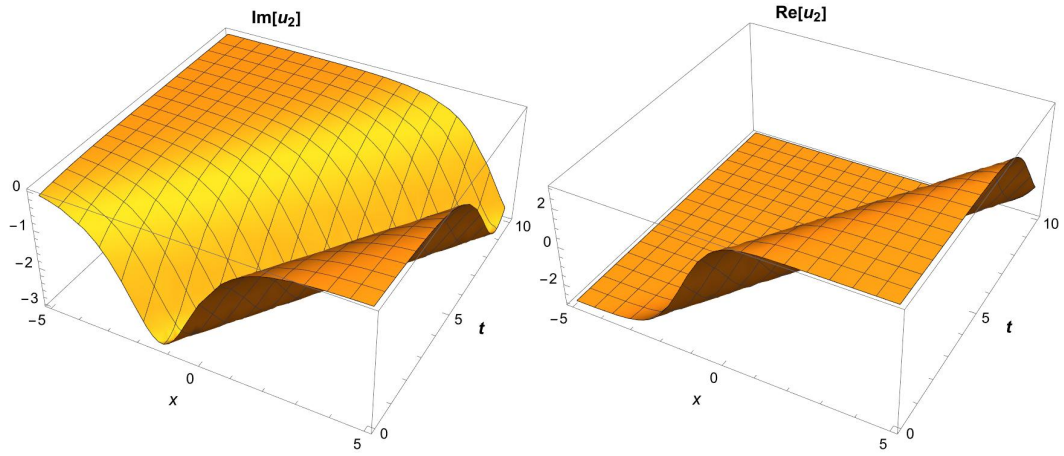

Figure 8. Three-dimensional wave behavior of Eq (4.20) for the specified values $k = 2, A_1 = 3, c = 0.2, a = 0.23, y = 1$, and $\beta = 0.99$.

Case 3. Considering the coefficients

$$A_0 = 0, B_1 = iA_1, k = 1 - \frac{3w}{aA_1^2}, c = 3b + 2w - \frac{3bw}{aA_1^2} + \frac{2aA_1^2}{3} + \frac{3w(b+2w)}{-3w + aA_1^2}, \tag{4.21}$$

then we arrive at another complex solution for Eq (1.2) as shown below

$$\begin{aligned} u_3(x,y,t) = A_1\Bigg(i\,\mathrm{sech}\left[x + y + \frac{w\left(t + \frac{1}{\Gamma(\beta)}\right)^{\beta}}{\beta} - \frac{3yw}{aA_1^2}\right] + \\ \tanh\left[x + y + \frac{w\left(t + \frac{1}{\Gamma(\beta)}\right)^{\beta}}{\beta} - \frac{3yw}{aA_1^2}\right]\Bigg), \end{aligned} \tag{4.22}$$

where $0 < \beta \leq 1$. The 2D dynamics of the complex solution u_3 in Eq (4.22) is visualized in Figure 9, which illustrates the imaginary and the real components. The imaginary part exhibits a soliton-like localized peak centered around $x \approx -2$, which decays symmetrically on both sides. On the other hand, the real part shows a smooth kink-like transition across $x = 0$, representing a wave front or domain wall.

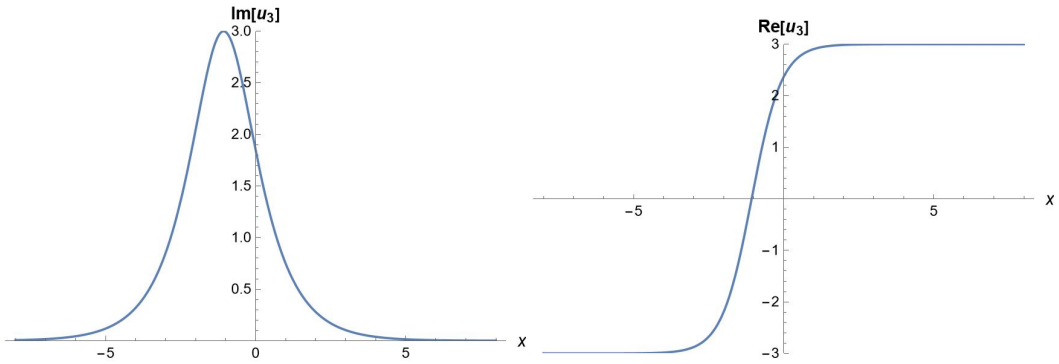

Figure 9. The 2D dynamics of Eq (4.22) for $k = 2, A_1 = 3, y = 1, a = 0.3, w = 0.23$, and $\beta = 0.99$.

4.3. RSGEM solution of the (2+1)-dimensional gKdV equation

In Eq (4.3), we select $N = M = 1$, and then the test function for the solution can be written as follows:

$$U(w) = \frac{A_0 + A_1 \sin(w) + c_1 \cos(w)}{B_0 + B_1 \sin(w) + d_1 \cos(w)}, \tag{4.23}$$

where $A_0 \neq B_0$, $A_1 \neq B_1$, and $c_1 \neq d_1$ simultaneously, with the condition that neither B_1 nor d_1 can be zero at the same time. If $A_0 = B_0$, $A_1 = B_1$, and $c_1 = d_1$, then the solution becomes trivial. By substituting Eq (4.23) into (4.3), we derive an algebraic equation involving trigonometric functions of varying orders. By equating the coefficients of terms with the same powers, we obtain a system of equations. By solving this system using Wolfram Mathematical 14, we obtain the following set of results.

Set 1. The first set of results is presented as follows:

$$\begin{aligned} &A_1 = -\frac{A_0 B_0 \sqrt{B_0^2 - d_1^2} - 3\sqrt{A_0^2 B_0^2 (B_0^2 - d_1^2)}}{2B_0^2}, B_1 = \sqrt{B_0^2 - d_1^2}, b = \frac{c(-1+k)k + w}{-1+k^3}, \\ &a = -\frac{2wB_0}{(-1+k)A_0}, c_1 = \frac{A_0 d_1}{B_0}. \end{aligned} \tag{4.24}$$

From (3.14) and (4.24), the mixed hyperbolic traveling wave solution of Eq (1.1) is as follows:

$$u_1(x,y,t) = \frac{A_0 + A_1 \operatorname{sech}\left[x + ky + \frac{1}{\beta} w\left(t + \frac{1}{\Gamma(\beta)}\right)^{\beta}\right] + \frac{A_0 d_1}{B_0} \tanh\left[x + ky + \frac{1}{\beta} w\left(t + \frac{1}{\Gamma(\beta)}\right)^{\beta}\right]}{B_0 + \operatorname{sech}\left[x + ky + \frac{1}{\beta} w\left(t + \frac{1}{\Gamma(\beta)}\right)^{\beta}\right] \sqrt{B_0^2 - d_1^2} + d_1 \tanh\left[x + ky + \frac{1}{\beta} w\left(t + \frac{1}{\Gamma(\beta)}\right)^{\beta}\right]}, \tag{4.25}$$

where $A_0 \neq 0, B_0 \neq 0, d_1 \neq 0$, and $0 < \beta \leq 1$ for the valid solution. Various simulations of Eq (4.25) are illustrated in Figure 10.

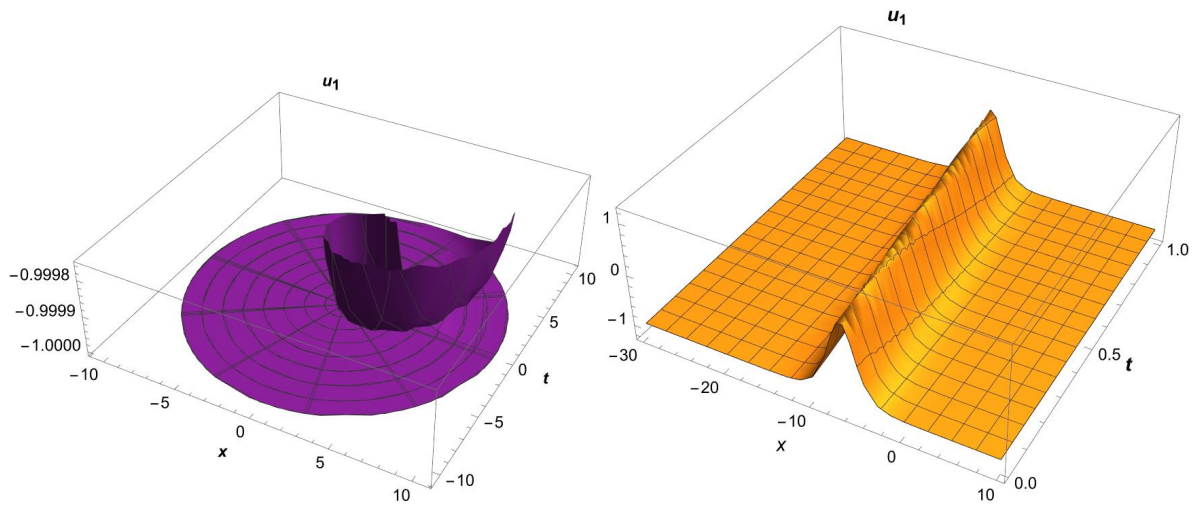

Figure 10. Revolutionary and 3D wave behaviors of Eq (4.25) are shown for the parameter values $A_0 = -2, B_0 = 2, k = 2, d_1 = 1, y = 1, w = 4$, and $\beta = 0.9$.

Set 2. The second result is given by

$$A_0 = \frac{1}{4}A_1B_0\left(-\frac{1}{\sqrt{B_0^2-d_1^2}}-\frac{3A_1d_1}{\sqrt{A_1^2d_1^2(B_0^2-d_1^2)}}\right), B_1 = -\sqrt{B_0^2-d_1^2},$$
$$w = (-1+k)(-ck+b(1+k+k^2)), c_1 = \frac{A_1d_1\sqrt{B_0^2-d_1^2}+3\sqrt{A_1^2d_1^2(B_0^2-d_1^2)}}{4(-B_0^2+d_1^2)}, \tag{4.26}$$
$$a = \frac{4(-ck+b(1+k+k^2))-(B_0^2+d_1^2)(-A_1d_1\sqrt{B_0^2-d_1^2}+\sqrt{A_1^2d_1^2(B_0^2-d_1^2)})}{A_1(\sqrt{B_0^2-d_1^2}\sqrt{A_1^2d_1^2(B_0^2-d_1^2)})+A_1(-B_0^2d_1+d_1^3))}.$$

From (3.14) and (4.26), the mixed hyperbolic traveling wave solution for Eq (1.1) is expressed as follows:

$$\begin{aligned}
&u_2(x,y,t) = \\
&\left(\operatorname{sech}\left[x+ky+\frac{1}{\beta}(-1+k)(-ck+b(1+k+k^2))\left(t+\frac{1}{\Gamma(\beta)}\right)^{\beta}\right]A_1+\right. \\
&\frac{1}{4}A_1B_0\left(-\frac{1}{\sqrt{B_0^2-d_1^2}}-\frac{3A_1d_1}{\sqrt{A_1^2d_1^2(B_0^2-d_1^2)}}\right)+ \\
&\left.\frac{(A_1d_1\sqrt{B_0^2-d_1^2}+3\sqrt{A_1^2d_1^2(B_0^2-d_1^2)})\tanh\left[x+ky+\frac{1}{\beta}(-1+k)(-ck+b(1+k+k^2))\left(t+\frac{1}{\Gamma(\beta)}\right)^{\beta}\right]}{4(-B_0^2+d_1^2)}\right)\Bigg/ \\
&\left(B_0-\operatorname{sech}\left[x+ky+\frac{1}{\beta}(-1+k)(-ck+b(1+k+k^2))\left(t+\frac{1}{\Gamma(\beta)}\right)^{\beta}\right]\sqrt{B_0^2-d_1^2}+\right. \\
&\left.d_1\tanh\left[x+ky+\frac{1}{\beta}(-1+k)(-ck+b(1+k+k^2))\left(t+\frac{1}{\Gamma(\beta)}\right)^{\beta}\right]\right),
\end{aligned} \tag{4.27}$$

where $A_0 \neq 0, B_0 \neq 0, d_1 \neq 0$, and $0 < \beta \leq 1$ for the valid solution.

Set 3. The third result is provided by

$$\begin{aligned}
A_1 &= -2\sqrt{A_0^2-c_1^2}, \\
k &= \frac{(-b+c)B_0-\sqrt{B_0(-2abA_0-(3b-c)(b+c)B_0)}}{2bB_0}, \\
B_1 &= \frac{B_0\sqrt{A_0^2-c_1^2}}{A_0}, d_1 = \frac{B_0c_1}{A_0}, \\
w &= \frac{aA_0\left((3b-c)B_0+\sqrt{B_0(-2abA_0-(3b-c)(b+c)B_0)}\right)}{4bB_0^2}.
\end{aligned} \tag{4.28}$$

Using (3.14) and (4.28), the mixed hyperbolic traveling wave solution for Eq (1.1) can be written as

$$
\begin{aligned}
&u_3(x,y,t) = \\
&\Bigg(A_0 - 2\,\mathrm{sech}\Bigg[x + \frac{y((-b+c)B_0 - \sqrt{B_0(-2abA_0 - (3b-c)(b+c)B_0)})}{2bB_0} + \\
&\frac{a(t+\frac{1}{\Gamma(\beta)})^{\beta}A_0((3b-c)B_0 + \sqrt{B_0(-2abA_0 - (3b-c)(b+c)B_0)})}{4b\beta B_0^2}\Bigg]\sqrt{A_0^2 - c_1^2} + \\
&c_1 \tanh\Bigg[x + \frac{y((-b+c)B_0 - \sqrt{B_0(-2abA_0 - (3b-c)(b+c)B_0)})}{2bB_0} + \\
&\frac{a(t+\frac{1}{\Gamma(\beta)})^{\beta}A_0((3b-c)B_0 + \sqrt{B_0(-2abA_0 - (3b-c)(b+c)B_0)})}{4b\beta B_0^2}\Bigg]\Bigg)\Big/ \\
&\Bigg(B_0 + \frac{1}{A_0}\,\mathrm{sech}\Bigg[x + \frac{y((-b+c)B_0 - \sqrt{B_0(-2abA_0 - (3b-c)(b+c)B_0)})}{2bB_0} + \\
&\frac{a(t+\frac{1}{\Gamma(\beta)})^{\beta}A_0((3b-c)B_0 + \sqrt{B_0(-2abA_0 - (3b-c)(b+c)B_0)})}{4b\beta B_0^2}\Bigg]B_0\sqrt{A_0^2 - c_1^2} + \\
&\frac{1}{A_0}B_0c_1 \tanh\Bigg[x + \frac{y((-b+c)B_0 - \sqrt{B_0(-2abA_0 - (3b-c)(b+c)B_0)})}{2bB_0} + \\
&\frac{a(t+\frac{1}{\Gamma(\beta)})^{\beta}A_0((3b-c)B_0 + \sqrt{B_0(-2abA_0 - (3b-c)(b+c)B_0)})}{4b\beta B_0^2}\Bigg]\Bigg),
\end{aligned}
\tag{4.29}
$$

where $A_0 \neq 0, B_0 \neq 0, d_1 \neq 0$, and $0 < \beta \leq 1$ for the valid solution.

Set 4. The fourth result is presented by

$$
\begin{aligned}
&A_1 = 2\sqrt{A_0^2 - c_1^2}, B_0 = -\frac{A_0B_1}{\sqrt{A_0^2 - c_1^2}}, d_1 = -\frac{B_1c_1}{\sqrt{A_0^2 - c_1^2}}, \\
&a = \frac{2(-ck + b(1+k+k^2))B_1}{\sqrt{A_0^2 - c_1^2}}, w = (-1+k)(-ck + b(1+k+k^2)).
\end{aligned}
\tag{4.30}
$$

Utilizing (3.14) and (4.30), the mixed hyperbolic traveling wave solution for Eq (1.1) is given as

$$
\begin{aligned}
&U_4(x,y,t) = \\
&\Bigg(A_0 + 2\,\mathrm{sech}\Bigg[x + ky + \frac{1}{\beta}(-1+k)(-ck + b(1+k+k^2))\Big(t + \frac{1}{\Gamma(\beta)}\Big)^{\beta}\Bigg]\sqrt{A_0^2 - c_1^2} + \\
&c_1 \tanh\Bigg[x + ky + \frac{1}{\beta}(-1+k)(-ck + b(1+k+k^2))\Big(t + \frac{1}{\Gamma(\beta)}\Big)^{\beta}\Bigg]\Bigg)\Big/ \\
&\Bigg(\mathrm{sech}\Bigg[x + ky + \frac{1}{\beta}(-1+k)(-ck + b(1+k+k^2))\Big(t + \frac{1}{\Gamma(\beta)}\Big)^{\beta}\Bigg]B_1 - \\
&\frac{A_0B_1}{\sqrt{A_0^2 - c_1^2}} - \frac{B_1c_1}{\sqrt{A_0^2 - c_1^2}} \tanh\Bigg[x + ky + \frac{1}{\beta}(-1+k)(-ck + b(1+k+k^2))\Big(t + \frac{1}{\Gamma(\beta)}\Big)^{\beta}\Bigg]\Bigg),
\end{aligned}
\tag{4.31}
$$

where $A_0 \neq 0, B_0 \neq 0, d_1 \neq 0$, and $0 < \beta \leq 1$ for the valid solution.

4.4. RSGEM solution of the (2+1)-dimensional mKdV equation

For Eq (4.15), we choose $N = M = 1$, allowing the test function for the solution to be formulated as

$$U(w) = \frac{A_0 + A_1 \sin(w) + c_1 \cos(w)}{B_0 + B_1 \sin(w) + d_1 \cos(w)}, \tag{4.32}$$

where $A_0 \neq B_0$, $A_1 \neq B_1$, and $c_1 \neq d_1$, while ensuring that neither that neither B_1 nor d_1 is zero simultaneously. If $A_0 = B_0$, $A_1 = B_1$, and $c_1 = d_1$, then the solution simplifies to a trivial form. By substituting Eq (4.32) into (4.15), we generate an algebraic equation involving trigonometric terms of different orders. Aligning the coefficients of terms with equivalent powers results in a system of equations. Solving this system computationally yields the following outcomes.

Set 1. If we select the coefficients

$$A_0 = -\frac{iA_1 d_1}{B_0}, B_1 = id_1, b = \frac{c(-1+k)k + 2w}{-1+k^3}, a = \frac{3wB_0^2}{(-1+k)A_1^2}, c = -iA_1, \tag{4.33}$$

we obtain the following solution in the form of a mixed hyperbolic function:

$$u_1(x,y,t) = -\frac{iA_1}{d_1}\left(1 + \frac{-B_0^2 d_1^2}{B_0\left(B_0 + d_1\left(i\,\mathrm{sech}\left[x + ky + \frac{w}{\beta}\left(t + \frac{1}{\Gamma(\beta)}\right)^{\beta}\right] + \tanh\left[x + ky + \frac{w}{\beta}\left(t + \frac{1}{\Gamma(\beta)}\right)^{\beta}\right]\right)\right)}\right), \tag{4.34}$$

where $A_0 \neq 0, B_0 \neq 0, d_1 \neq 0$, and $0 < \beta \leq 1$ for the valid solution. Various graphs of Eq (4.34) are displayed in Figure 11.

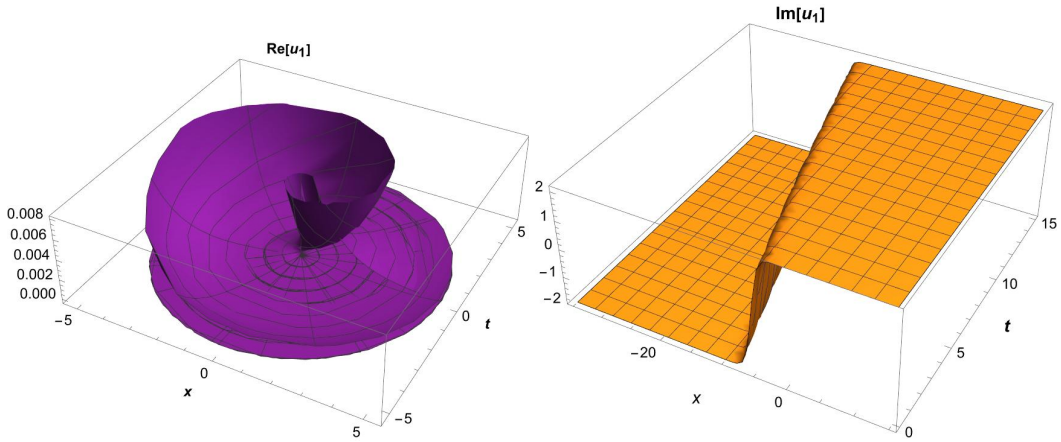

Figure 11. Revolutionary and 3D wave behaviors of Eq (4.34) are shown for the parameter values $A_1 = -2, B_0 = 1, k = 2, d_1 = 3, y = 2, w = 1$, and $\beta = 0.9$.

Set 2. Considering

$$A_1 = \frac{iA_0\sqrt{B_0^2 - B_1^2 - d_1^2}}{d_1}, b = \frac{c(-1+k)k + 2w}{-1+k^3}, a = -\frac{3wd_1^2}{(-1+k)A_0^2}, c_1 = \frac{A_0 B_0}{d_1}, \tag{4.35}$$

yields the following solution in terms of mixed hyperbolic functions:

$$u_2(x,y,t) = \frac{A_0\left(d_1 + i\,\mathrm{sech}\left[x+ky+\frac{w}{\beta}\left(t+\frac{1}{\Gamma(\beta)}\right)^{\beta}\right]\sqrt{B_0^2-B_1^2-d_1^2} + B_0\tanh\left[x+ky+\frac{w}{\beta}\left(t+\frac{1}{\Gamma(\beta)}\right)^{\beta}\right]\right)}{d_1\left(B_0+\mathrm{sech}\left[x+ky+\frac{w}{\beta}\left(t+\frac{1}{\Gamma(\beta)}\right)^{\beta}\right]B_1 + d_1\tanh\left[x+ky+\frac{w}{\beta}\left(t+\frac{1}{\Gamma(\beta)}\right)^{\beta}\right]\right)}, \tag{4.36}$$

where $A_0 \neq 0, B_0 \neq 0, d_1 \neq 0, B_0^2 \neq B_1^2 + d_1^2$, and $0 < \beta \leq 1$ for the valid solution. Various graphs of Eq (4.36) are shown in Figures 12 and 13.

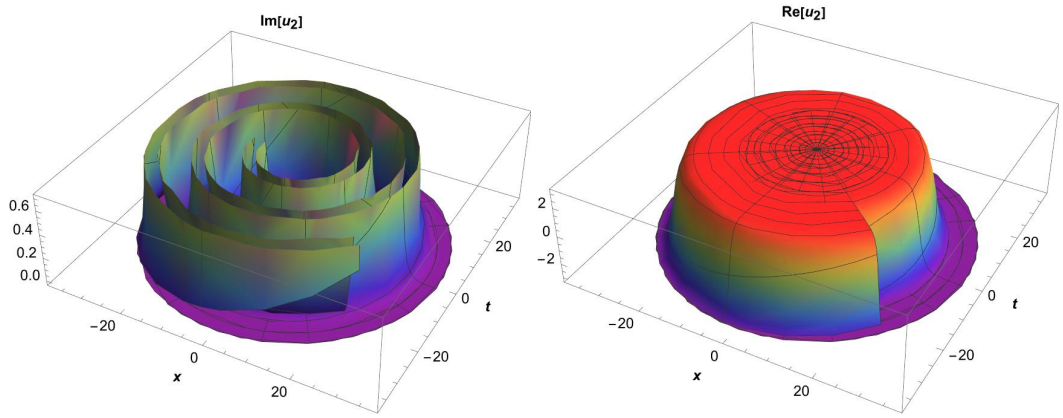

Figure 12. Revolutionary wave behaviors of Eq (4.36) are shown for the parameter values $A_0 = 3, w = 2, B_0 = 3, k = 2, d_1 = 1, y = 3, A_1 = 2, B_1 = 2$, and $\beta = 0.9$.

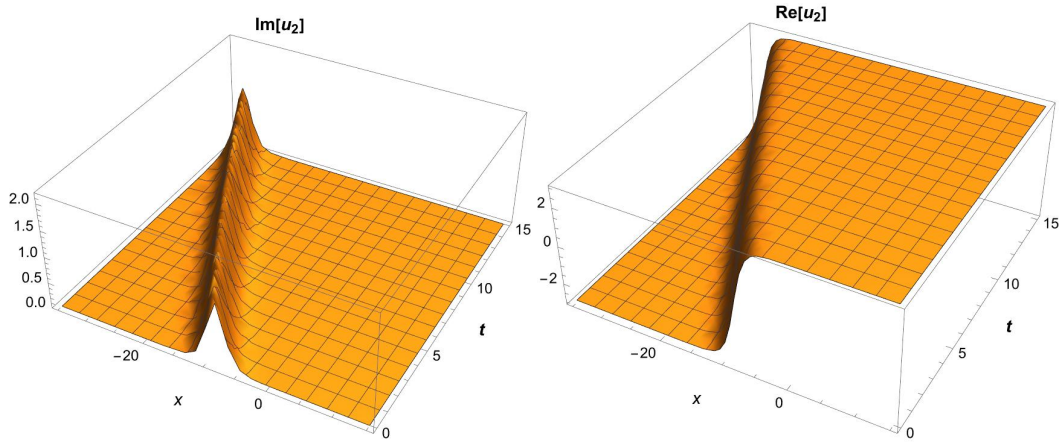

Figure 13. Three-dimensional wave behaviors of Eq (4.36) are shown for the parameter values $A_0 = 3, w = 2, B_0 = 3, k = 2, d_1 = 1, y = 3, A_1 = 2, B_1 = 2$, and $\beta = 0.9$.

Set 3. Selecting the coefficients

$$A_1 = -\frac{iA_0\sqrt{B_0^2-d_1^2}}{d_1}, B_1 = 0, b = \frac{c(-1+k)k+2w}{-1+k^3}, a = -\frac{3wd_1^2}{(-1+k)A_0^2}, c_1 = \frac{A_0B_0}{d_1}, \tag{4.37}$$

produces the following solution in the form of mixed hyperbolic functions:

$$u_3(x,y,t) = \frac{A_0\left(d_1 - i\,\mathrm{sech}\left[x+ky+\frac{w}{\beta}\left(t+\frac{1}{\Gamma(\beta)}\right)^{\beta}\right]\sqrt{B_0^2-d_1^2} + B_0\tanh\left[x+ky+\frac{w}{\beta}\left(t+\frac{1}{\Gamma(\beta)}\right)^{\beta}\right]\right)}{d_1\left(B_0 + d_1\tanh\left[x+ky+\frac{w}{\beta}\left(t+\frac{1}{\Gamma(\beta)}\right)^{\beta}\right]\right)}, \tag{4.38}$$

where $A_0 \neq 0, B_0 \neq 0, d_1 \neq 0, B_0^2 \neq d_1^2$, and $0 < \beta \leq 1$ for the valid solution. Various graphs of Eq (4.38) are shown in Figure 14.

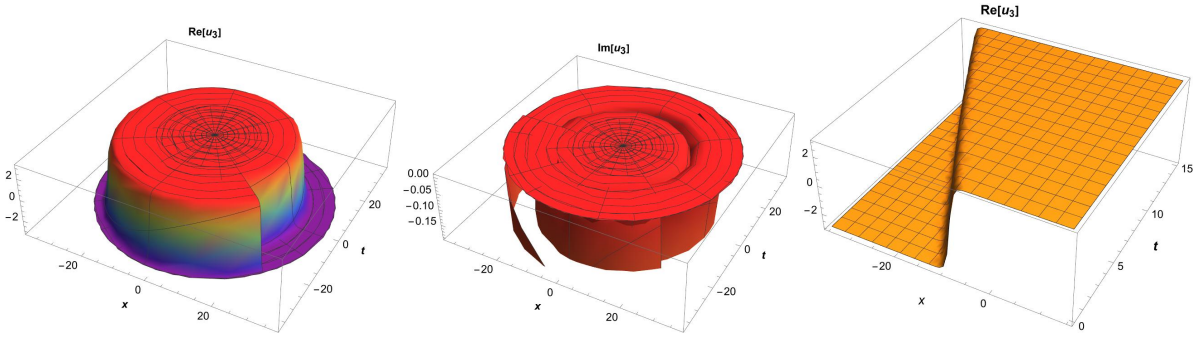

Figure 14. Revolutionary and 3D wave behaviors of Eq (4.38) are illustrated using the parameter values $A_0 = 3, w = 2, B_0 = 3, k = 2, d_1 = 1, y = 3$, and $\beta = 0.9$.

5. Results and discussion

The analytical solutions derived using SGEM and RSGEM methods, presented in Sections 4, provide significant insights into the behavior of nonlinear systems. These solutions encompass diverse forms, including hyperbolic, trigonometric, exponential, and mixed solutions, and their behaviors are depicted through a series of revolutionary and 3D figures. The waveforms thus obtained, such as solitary and periodic waves, represent fundamental solutions in nonlinear dynamics. For instance, the hyperbolic solutions visualized in Figure 3 exhibit localized wave structures resembling solitons, which are crucial for understanding phenomena like shallow-water wave propagation and plasma turbulence. These solutions underscore the capability of the SGEM in modeling systems with minimal dispersion effects. The results highlight the influence of parameters such as A_0, B_0, k, and β. For example, in Figures 12–14, varying the parameter β demonstrates its role in controlling waves' steepness and amplitude. Higher values of β result in smoother wave profiles, indicating the adaptability of the RSGEM to capture different physical conditions. The mixed hyperbolic traveling wave solutions derived via the RSGEM provide a richer dynamic range compared with the standard trigonometric solutions of the SGEM. As illustrated in Figure 10, the rational forms incorporate amplitude modulation and phase shifts, enabling a detailed exploration of complex wave interactions in nonlinear systems. This contrast emphasizes the extended capabilities of the RSGEM. The stability of these solutions aligns with the governing equations, demonstrating their robustness for modeling various physical phenomena. Applications of these solutions include modeling optical solitons in fiber optics, acoustic wave propagation in non-uniform atmospheric layers, and energy transfer mechanisms

in nonlinear systems. The exponential solutions, such as those in Eqs (4.25) and (4.34), offer potential for describing rapid energy transfer processes. The simulations in Figures 1–14 not only validate the solutions but also provide a visual representation of their dynamics. For instance, Figure 6 highlights the transition from localized wave structures to periodic patterns under specific parameter settings, offering insights into the interplay of nonlinear effects and dispersion.

6. Conclusions

In this paper, we first presented the general properties of recently developed the SGEM and RSGEM for constructing analytic solutions to Eqs (1.1) and (1.2). The RSGEM extends the SGEM by incorporating the two main properties of the sine-Gordon equation. Using both, the SGEM and RSGEM, a detailed investigation of the nonlinear (2+1)-dimensional gKdV and mKdV equations was conducted. These methods are capable of generating a variety of solutions, including traveling waves, periodic waves, and solitary wave solutions. We applied the SGEM to the generalized forms of the (2+1)-dimensional gKdV and mKdV equations, which play a crucial role in modeling shallow-water waves. Through this method, we conducted a detailed investigation of the nonlinear (2+1)-dimensional gKdV and mKdV equations. Using the SGEM and RSGEM, we derived several new solutions, including complex, trigonometric, exponential, and mixed hyperbolic function solutions for the gKdV and mKdV equations, as shown in Eqs (4.6), (4.8), (4.10), (4.12), (4.18), (4.20), and (4.22). These new solutions are inherent to the general properties of the SGEM and contribute to understanding the dynamic behavior of various scientific phenomena, such as water waves, solitons, and explosive processes. Alongside these wave solutions, we obtained the exponential function solutions given in Eqs (4.25), (4.27), (4.34), and (4.36), which differ from the SGEM results. These additional solutions come from the unique properties of the RSGEM. Furthermore, we verified that all the solutions satisfied the nonlinear (2+1)-dimensional gKdV equation (1.1) and mKdV equation (1.2). We also presented simulations of these solutions based on different parameter values, with the results illustrated through 3D, 2D, and revolutionary plots. The figures and results reveal significant properties of the generalized KdV and mKdV models, including complex, hyperbolic, exponential, and mixed hyperbolic solutions. It is estimated that these solutions of $u(x, y, t)$ may provide valuable insights into interactions between long waves with well-defined dispersion relationships. The results and corresponding graphs provide a comprehensive evaluation of the SGEM and RSGEM, demonstrating that these are an effective and flexible method for obtaining analytic solutions for a broad class of NLPDEs. As such, they are well-suited for addressing a wide range of scientific and engineering problems. Additionally, the findings presented in this paper highlight the potential of the proposed method for application in other areas of study.

Author contributions

Yaya Wang: Writing-review & editing, Supervision, Validation; Md Nurul Raihen: Writing-original draft, Writing-review and editing, Validation, Software; Haci Mehmet Baskonus: Methodology, Supervision, Validation, Conceptualization, Formal analysis; Esin Ilhan: Review & editing, Software. All authors read and approved the final submitted version of this manuscript.

Use of Generative-AI tools declaration

The authors declare they have not used Artificial Intelligence (AI) tools in the creation of this article.

Acknowledgments

The authors deeply appreciate the reviewers for their helpful and constructive suggestions, which helped further improve this paper.

The second author thanks to Harran University due to their support via a Postdoc position.

Conflict of interest

The authors hereby declare that there is no conflict of interests regarding the publication of this paper.

References

1. T. Roubíček, *Nonlinear partial differential equations with applications*, Springer Science & Business Media, **153** (2013). https://doi.org/10.1007/978-3-0348-0513-1
2. A. W. Leung, *Systems of nonlinear partial differential equations: Applications to biology and engineering*, Springer Science & Business Media, **49** (2013). https://doi.org/10.1007/978-94-015-3937-1
3. A. Cheviakov, P. Zhao, *Analytical properties of nonlinear partial differential equations: With applications to shallow water models*, Springer Nature, **10** (2024). https://doi.org/10.1007/978-3-031-53074-6
4. F. Z. Wang, M. M. A. Khater, Computational simulation and nonlinear vibration motions of isolated waves localized in small part of space, *J. Ocean Eng. Sci.*, 2022. https://doi.org/10.1016/j.joes.2022.03.009
5. B. C. Li, F. Z. Wang, S. Nadeem, Explicit and exact travelling wave solutions for Hirota equation and computerized mechanization, *Plos One*, **5** (2024), e0303982. https://doi.org/10.1371/journal.pone.0303982
6. D. J. Korteweg, G. de Vries, On the change of form of long waves advancing in a rectangular canal, and on a new type of long stationary waves, In: *The London, Edinburgh, and Dublin Philosophical Magazine and Journal of Science*, **39** (1895), 422–443. https://doi.org/10.1080/14786449508620739
7. Y. R. Xia, W. J. Huang, R. X. Yao, Y. Li, Nonlinear superposition and trajectory equations of lump soliton with other nonlinear localized waves for (2+1)-dimensional nonlinear wave equation, *Nonlinear Dyn.*, 2024, 1–19. https://doi.org/10.1007/s11071-024-10685-w
8. Y. R. Xia, R. X. Yao, X. P. Xin, Y. Li, Trajectory equation of a lump before and after collision with other waves for (2+1)-dimensional Sawada-Kotera equation, *Appl. Math. Lett.*, **135** (2023), 108408. https://doi.org/10.1016/j.aml.2022.108408

9. S. Sivasundaram, A. Kumar, R. K. Singh, On the complex properties to the first equation of the Kadomtsev-Petviashvili hierarchy, *Int. J. Math. Comput. Eng.*, **2** (2024), 71–84. https://doi.org/10.2478/ijmce-2024-0006
10. M. Bendahmane, Y. Ouakrim, Y. Ouzrour, M. Zagour, Mathematical study of a new coupled electro-thermo radiofrequency model of cardiac tissue, *Commun. Nonlinear Sci. Numer. Simulat.*, **139** (2024), 108281. https://doi.org/10.1016/j.cnsns.2024.108281
11. Y. H. Zheng, Optimization of computer programming based on mathematical models of artificial intelligence algorithms, *Comput. Electr. Eng.*, **110** (2023), 108834. https://doi.org/10.1016/j.compeleceng.2023.108834
12. Z. Sabir, M. Umar, Levenberg-Marquardt backpropagation neural network procedures for the consumption of hard water-based kidney function, *Int. J. Math. Comput. Eng.*, **1** (2023), 127–138. https://doi.org/10.2478/ijmce-2023-0010
13. R. Kumar, S. Dhua, Dynamic analysis of Hashimoto's Thyroiditis bio-mathematical model using artificial neural network, *Math. Comput. Simulat.*, **229** (2025), 235–245. https://doi.org/10.1016/j.matcom.2024.10.001
14. W. G. Hao, X. Y. Wang, J. J. Ma, P. Gong, L. Wang, Operation prediction of open sun drying based on mathematical-physical model, drying kinetics and machine learning, *Innov. Food Sci. Emerg. Tech.*, **97** (2024), 103836. https://doi.org/10.1016/j.ifset.2024.103836
15. J. L. G. Guirao, On the stochastic observation for the nonlinear system of the emigration and migration effects via artificial neural networks, *Int. J. Math. Comput. Eng.*, **1** (2023), 177–186. https://doi.org/10.2478/ijmce-2023-0014
16. R. Zarin, N. Ullah, A. Khan, U. W. Humphries, A numerical study of a new non-linear fractal fractional mathematical model of malicious codes propagation in wireless sensor networks, *Comput. Secur.*, **135** (2023), 103484. https://doi.org/10.1016/j.cose.2023.103484
17. M. A. Basit, M. Imran, W. W. Mohammed, M. R. Ali, A. S. Hendy, Thermal Analysis of Mathematical Model of Heat and Mass Transfer through Bioconvective Carreau Nanofluid Flow over an Inclined Stretchable Cylinder, *Case Stud. Therm. Eng.*, **63** (2024), 105303. https://doi.org/10.1016/j.csite.2024.105303
18. R. Pandey, G. R. Jayanth, M. S. M. Kumar, Comprehensive mathematical model for efficient and robust control of irrigation canals, *Environ. Modell. Softw.*, **178** (2024), 106083. https://doi.org/10.1016/j.envsoft.2024.106083
19. J. E. A. McIntosh, R. P. McIntosh, *Mathematical modelling and computers in endocrinology*, Monographs on Endocrinology, **16** (1980), 1–337. https://doi.org/10.1007/978-3-642-81401-3
20. L. J. Yang, Q. K. Song, Y. R. Liu, Dynamics analysis of a new fractional-order SVEIR-KS model for computer virus propagation: Stability and Hopf bifurcation, *Neurocomputing*, **598** (2024), 128075. https://doi.org/10.1016/j.neucom.2024.128075
21. A. H. Seddik, M. Salah, G. Behery, A. E. harby, A. I. Ebada, S. Teng, et al., A new generative mathematical model for coverless steganography system based on image generation, *Comput. Mater. Con.*, **74** (2023), 5087–5103. https://doi.org/10.32604/cmc.2023.035364

22. M. Pompa, A. D. Gaetano, A. Borri, A. Farsetti, S. Nanni, A. Pontecorvi, et al., A physiological mathematical model of the human thyroid, *J. Comput. Sci.*, **76** (2024), 102236. https://doi.org/10.1016/j.jocs.2024.102236

23. Z. Szymańska, M. Lachowicz, N. Sfakianakis, M. A. J. Chaplain, Mathematical modelling of cancer invasion: Phenotypic transitioning provides insight into multifocal foci formation, *J. Comput. Sci.*, **75** (2024), 102175. https://doi.org/10.1016/j.jocs.2023.102175

24. G. D. Lu, A. P. S. Selvadurai, M. A. Meguid, Analytical solution to non-isothermal pore-pressure evolution in hydrating minefill, *Can. Geotech. J.*, **61** (2024), 2722–2734. https://doi.org/10.1139/cgj-2023-0464

25. H. J. Jiang, Q. Z. Guo, X. G. Wang, N. H. Gao, Analytical solution of three-dimensional temperature field for skin tissue considering blood perfusion rates under laser irradiation and thermal damage analysis, *Optik*, **312** (2024), 171982. https://doi.org/10.1016/j.ijleo.2024.171982

26. N. H. Sweilam, S. M. A. Mekhlafi, W. S. A. Kareem, G. Alqurishi, A new crossover dynamics mathematical model of monkeypox disease based on fractional differential equations and the Ψ Caputo derivative: Numerical treatments, *Alex. Eng. J.*, **111** (2025), 181–193. https://doi.org/10.1016/j.aej.2024.10.019

27. U. Shirole, M. Joshi, Prediction of left ventricle ejection fraction from HRV in diabetics and cardiac diseased subjects: A mathematical model approach, *Med. Novel Tech. Dev.*, **23** (2024), 100317. https://doi.org/10.1016/j.medntd.2024.100317

28. X. Y. Gao, In plasma physics and fluid dynamics: Symbolic computation on a (2+1)-dimensional variable-coefficient Sawada-Kotera system, *Appl. Mathh. Lett.*, **159** (2025), 109262. https://doi.org/10.1016/j.aml.2024.109262

29. X. T. Gao, B. Tian., Similarity reductions on a (2+1)-dimensional variable-coefficient modified Kadomtsev-Petviashvili system describing certain electromagnetic waves in a thin film, *Int. J. Theor. Phys.*, **63** (2024), 99. https://doi.org/10.1007/s10773-024-05629-4

30. B. Kemaloğlu, G. Yel, H. Bulut, An application of the rational sine-Gordon method to the Hirota equation, *Opt. Quant. Elecron.*, **55** (2023), 658. https://doi.org/10.1007/s11082-023-04930-6

31. A. A. Mahmud, Considerable traveling wave solutions of the generalized hietarinta-type equation, *Int. J. Math. Comput. Eng.*, **3** (2025), 185–200. https://doi.org/10.2478/ijmce-2025-0015

32. S. M. Ege, E. Misirli, A new method for solving nonlinear fractional differential equations, *New Trend. Math. Sci.*, **5** (2017), 225–233. http://dx.doi.org/10.20852/ntmsci.2017.141

33. G. W. Wang, A. H. Kara, A (2+1)-dimensional KdV equation and mKdV equation: Symmetries, group invariant solutions and conservation laws, *Phys. Lett. A*, **383** (2019), 728–731. https://doi.org/10.1016/j.physleta.2018.11.040

34. A. M. Wazwaz, New Painlevé-integrable (2+1)-and (3+1)-dimensional KdV and mKdV equations, *Romanian J. Phys.*, **65** (2020), 108.

35. S. Kumar, S. Malik, Soliton solutions of (2+1) and (3+1)-dimensional KdV and mKdV equations, *AIP Conf. Proc.*, **2435** (2022), 020027. https://doi.org/10.1063/5.0083653

36. R. R. Yuan, Y. Shi, S. L. Zhao, J. X. Zhao, The combined KdV-mKdV equation: Bilinear approach and rational solutions with free multi-parameters, *Result Phys.*, **55** (2023), 107188. https://doi.org/10.1016/j.rinp.2023.107188

37. N. H. Ali, S. A. Mohammed, J. Manafian, Study on the simplified MCH equation and the combined KdV-mKdV equations with solitary wave solutions, *Par. Diff. Eq. App. Math.*, **9** (2024), 100599. https://doi.org/10.1016/j.padiff.2023.100599

38. A. A. Boroujeni, R. Pourgholi, S. H. Tabasi, Numerical solutions of KDV and mKDV equations: Using sequence and multi-core parallelization implementation, *J. Comput. Appl. Math.*, **454** (2025), 116184. https://doi.org/10.1016/j.cam.2024.116184

39. A. A. Elmandouha, A. G. Ibrahim, Bifurcation and travelling wave solutions for a (2+1)-dimensional KdV equation, *J. Taibah Univ. Sci.*, **14** (2020), 139–147. https://doi.org/10.1080/16583655.2019.1709271

40. A. K. Gupta, S. S. Ray, On the solution of time-fractional KdV-Burgers equation using Petrov-Galerkin method for propagation of long wave in shallow water, *Chaos Solition. Fract.*, **116** (2018), 376–380. https://doi.org/10.1016/j.chaos.2018.09.046

41. G. W. Wang, A. M. Wazwaz, A new (3+1)-dimensional KdV equation and mKdV equation with their corresponding fractional forms, *Fractals*, **30** (2022), 2250081. https://doi.org/10.1142/S0218348X22500815

42. Y. Zhang, R. S. Ye, W. X. Ma, Binary Darboux transformation and soliton solutions for the coupled complex modified Korteweg-de Vries equations, *Math. Method Appl. Sci.*, **43** (2020), 613–627. https://doi.org/10.1002/mma.5914

43. N. A. Kudryashov, D. V. Safonova, Nonautonomous first integrals and general solutions of the KdV-Burgers and mKdV-Burgers equations with the source, *Math. Method Appl. Sci.*, **42** (2019), 4627–4636. https://doi.org/10.1002/mma.5684

44. A. Salas, S. Kumar, A. Yildirim, A. Biswas, Cnoidal waves, solitary waves and painleve analysis of the 5th order KdV equation with dual-power law nonlinearity, *Proceed. Romanian Aca., Series A*, **14** (2013), 28–34.

45. X. Y. Gao, In an ocean or a river: Bilinear auto-Bäcklund transformations and similarity reductions on an extended time-dependent (3+1)-dimensional shallow water wave equation, *China Ocean Eng.*, 2025. https://doi.org/10.1007/s13344-025-0012-y

46. X. Y. Gao, Hetro-Bäcklund transformation, bilinear forms and multi-solitons for a (2+1)-dimensional generalized modified dispersive water-wave system for the shallow water, *Chinese. J. Phys.*, **92** (2024), 1233–1239. https://doi.org/10.1016/j.cjph.2024.10.004

47. A. Atangana, D. Baleanu, A. Alsaedi, Analysis of time-fractional Hunter-Saxton equation: A model of neumatic liquid crystal, *Open Phys.*, **14** (2016), 145–149. https://doi.org/10.1515/phys-2016-0010

48. H. Y. Martínez, J. F. G. Aguilar, D. Baleanu, Beta-derivative and sub-equation method applied to the optical solitons in medium with parabolic law nonlinearity and higher order dispersion, *Optik*, **155** (2018), 357–365. https://doi.org/10.1016/j.ijleo.2017.10.104

49. K. Hosseini, M. Mirzazadeh, J. F. Gómez-Aguilar, Soliton solutions of the Sasa-Satsuma equation in the monomode optical fibers including the beta-derivatives, *Optik*, **224** (2020), 165425. https://doi.org/10.1016/j.ijleo.2020.165425

50. K. Hosseini, L. Kaur, M. Mirzazadeh, H. M. Baskonus, 1-soliton solutions of the (2+1)-dimensional Heisenberg ferromagnetic spin chain model with the beta time derivative, *Opt. Quant. Electron.*, **53** (2021), 125. https://doi.org/10.1007/s11082-021-02739-9

51. H. M. Baskonus, M. N. Raihen, M. Kayalar, On the extraction of complex behavior of generalized higher-order nonlinear Boussinesq dynamical wave equation and (1+1)-dimensional Van der Waals gas system, *AIMS Math.*, **9** (2024), 28379–28399. https://doi.org/10.3934/math.20241377

52. C. T. Yan, A simple transformation for nonlinear waves, *Phys. Lett. A*, **224** (1996), 77–84. https://doi.org/10.1016/S0375-9601(96)00770-0

53. H. M. Baskonus, New acoustic wave behaviors to the Davey-Stewartson equation with power-law nonlinearity arising in fluid dynamics, *Nonlinear Dyn.*, **86** (2016), 177–183. https://doi.org/10.1007/s11071-016-2880-4

AIMS Press